Sparse optical microstimulation in barrel cortex drives learned behaviour in freely moving mice

Daniel Huber[1,2], Leopoldo Petreanu[1,2], Nima Ghitani[1], Sachin Ranade[2], Tomáš Hromádka[2], Zach Mainen[2] & Karel Svoboda[1,2]

Electrical microstimulation can establish causal links between the activity of groups of neurons and perceptual and cognitive functions[1–6]. However, the number and identities of neurons microstimulated, as well as the number of action potentials evoked, are difficult to ascertain[7,8]. To address these issues we introduced the light-gated algal channel channelrhodopsin-2 (ChR2)[9] specifically into a small fraction of layer 2/3 neurons of the mouse primary somatosensory cortex. ChR2 photostimulation *in vivo* reliably generated stimulus-locked action potentials[10–13] at frequencies up to 50 Hz. Here we show that naive mice readily learned to detect brief trains of action potentials (five light pulses, 1 ms, 20 Hz). After training, mice could detect a photostimulus firing a single action potential in approximately 300 neurons. Even fewer neurons (approximately 60) were required for longer stimuli (five action potentials, 250 ms). Our results show that perceptual decisions and learning can be driven by extremely brief epochs of cortical activity in a sparse subset of supragranular cortical pyramidal neurons.

We used *in utero* electroporation[14] to introduce ChR2 fused to a green fluorescent protein (GFP) (ChR2–GFP[15]) together with a red fluorescent cytosolic marker[15] (RFP) into neocortical pyramidal neurons (Fig. 1a, Methods). In the adult brain, ChR2–GFP expression was restricted to pyramidal cells in layers 2/3 (more than 99.4%), mainly in the barrel cortex (Figs 1a and 2a). *In vivo* two-photon imaging and retrospective immunohistology revealed that ChR2–GFP was localized to the neuronal plasma membrane. ChR2–GFP was expressed in about half ($48.9 \pm 5.3\%$, $n = 10$, five mice; see Methods) of red fluorescent layer 2/3 neurons (Supplementary Movie 1). ChR2–GFP invaded the soma, dendrites and axons (Fig. 1b, c). ChR2–GFP expression was stable for at least 8 months and did not seem to perturb neuronal morphology (Fig. 1a–c, Methods).

We next characterized the responses of ChR2–GFP-expressing neurons to photostimulation in anaesthetized mice. To sample from the entire population of ChR2–GFP-expressing neurons, unbiased by ChR2–GFP expression level, we recorded from red fluorescent neurons using two-photon targeted loose-patch recordings[16] (Fig. 1c, d). Photostimuli consisted of light pulses, produced by a blue miniature light-emitting diode (LED; 470 nm), centred on the recording window (Fig. 1d). At maximum light intensities ($I_{max} = 11.6 \, \text{mW mm}^{-2}$ at the surface of the brain, centred on the diode; 1–10 ms duration) about half (51%) of the patched red neurons ($n = 39/77$, eight mice) responded reliably to single photostimuli with at most one action potential. Increasing the photostimulus duration beyond 10 ms did not reveal additional responsive neurons. The other half of the patched neurons did not fire spikes time-locked to the photostimuli, and presumably corresponded to ChR2–GFP-negative neurons. These measurements indicate that most ChR2–GFP-positive

neurons can be driven to spiking using our photostimulation system; furthermore, excitation of layer 2/3 neurons through indirect synaptic pathways was weak.
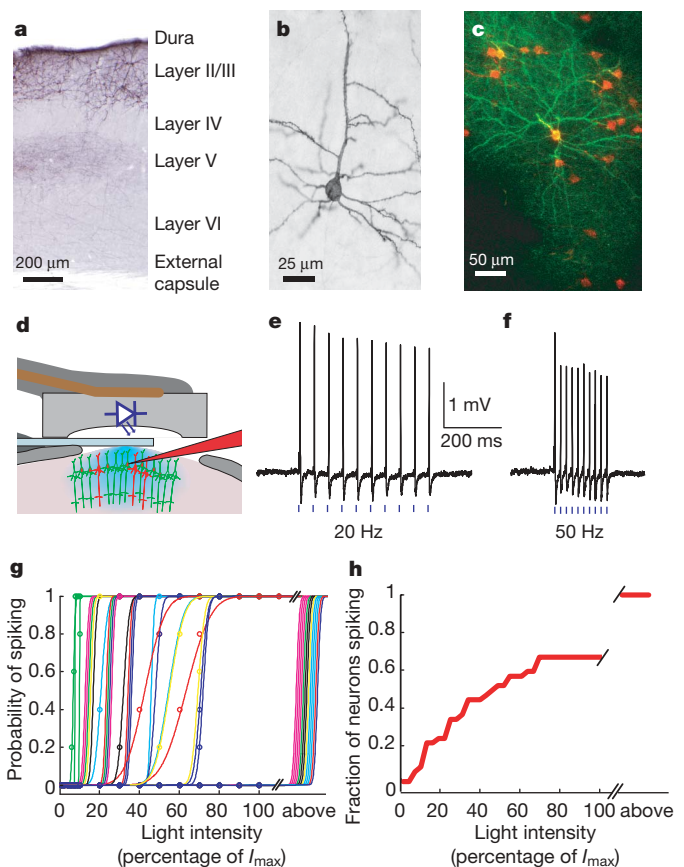

Figure 1 | ChR2-assisted photostimulation of layer 2/3 barrel cortex neurons *in vivo*. a, Coronal section through the electroporated mouse somatosensory cortex after immunohistochemical staining for ChR2–GFP. **b**, Individual layer 2/3 neuron, side view. **c**, Maximum value projection (top view) of an image stack *in vivo* (see Supplementary Movie 1) showing layer 2/3 neurons expressing ChR2–GFP and cytosolic RFP. **d**, Schematic of the recording geometry. **e**, Action potentials recorded from one ChR2–GFP-positive neuron. Blue bars indicate photostimuli (1 ms duration, 11.6 mW mm^{-2}, 20 Hz). **f**, Same as **e**, 50 Hz. **g**, Probability of spiking as a function of light intensity (1 ms duration, five repetitions per condition, 15 s between stimuli) ($I_{max} = 11.6 \, \text{mW mm}^{-2}$). Each line corresponds to a different neuron, each colour to a different animal. Neurons that could only be driven with photostimuli longer than 1 ms were pooled at the far right (above). **h**, Cumulative fraction of recorded neurons firing at various threshold intensity levels (computed from the data in **g**).

[1]Howard Hughes Medical Institute, Janelia Farm Research Campus, Ashburn, Virginia 20147, USA. [2]Cold Spring Harbor Laboratory, Cold Spring Harbor, New York 11724, USA.

When stimulated with 1 ms light pulses, ChR2–GFP-expressing neurons were able to follow frequencies up to 20 Hz (Fig. 1e) and in some cases up to 50 Hz (Fig. 1f). These frequencies are comparable to, or higher than, typical spike rates in the barrel cortex[17]. Action potentials followed the photostimuli with short delays (range 3–11 ms) and little jitter (Supplementary Fig. 1).

We next determined the relation between photostimulus intensity and the probability of spiking of ChR2–GFP-expressing neurons. During cell-attached recordings we stimulated with 1 ms light pulses while varying the photostimulus. With decreasing light intensity, neurons switched abruptly from firing action potentials with high probability to firing no action potentials. The photostimulus intensity required to trigger action potentials varied substantially across the population of ChR2–GFP-expressing neurons (Fig. 1g). Control experiments in brain slices revealed that the brightness of ChR2–GFP measured in individual cells was inversely correlated with firing threshold (Supplementary Fig. 2); in contrast, the firing threshold was independent of the depth of the recorded neuron *in vivo* (Supplementary Fig. 3). The variability in firing threshold in terms of photostimulus intensity therefore primarily reflects heterogeneity in the expression level of ChR2–GFP in individual neurons. These results confirm that ChR2 can transduce photostimuli into precisely timed spike trains *in vivo*[18]. Furthermore, the fraction of activated neurons can be tuned by modulating the excitation light intensity (Fig. 1h).

Can awake mice learn to report photostimulation of layer 2/3 pyramidal neurons in the barrel cortex? To address this question we delivered light pulses to ChR2–GFP-expressing neurons in freely moving animals (Fig. 2a). We first implanted a window above the barrel cortex[19], which provided optical access for photostimulation and screening the density of electroporated neurons. We next mounted the miniature LED centred on the imaging window (Fig. 2a; Methods). During the behavioural sessions the mice were temporarily connected to an LED controller (Methods). Mice were trained in a detection task to associate photostimulation of ChR2–GFP-expressing neurons (five light pulses, 20 Hz, 1 ms duration) with water reward on one of two choice ports (Fig. 2b, left port). After four to seven training sessions (200–800 trials per session) all animals expressing ChR2–GFP ($n = 9$) reliably reported photostimulation; in the presence (absence) of a photostimulus, mice chose the left (right) port (Fig. 3a, range 72–93% correct, defined as hits + correct rejections, divided by total number of trials; Supplementary Movie 2). Control mice without electroporated neurons ($n = 6$) performed at chance levels (50.1%, $P > 0.70$, t-test), even after 25 training sessions (Fig. 3a and Supplementary Fig. 4). These experiments demonstrate that photostimulation of layer 2/3 neurons can drive robust behaviour.

How many action potentials triggered by photostimulation are necessary for perception? To address this issue we further trained five mice to respond to one, two and five photostimuli at 20 Hz (example in Fig. 2c). Although performance decreased with fewer pulses, all ChR2–GFP-expressing mice were able to detect single action potentials in the activated cells, even at modest photostimulus intensities (Fig. 3b, red lines).

To determine the relation between performance and the number of neurons directly activated by light, we measured behaviour as a function of light intensity (Fig. 3b). As expected, behavioural performance decreased with decreasing photostimulus intensity, although the psychometric curves varied from animal to animal. For example, at the lowest intensities probed (10% of I_{max}) some animals continued to discriminate, whereas others performed at chance levels.

We counted the number of ChR2–GFP-positive somata and measured their positions (Fig. 3c; Methods). Between 594 and 1430 ChR2–GFP-positive neurons were found in a 2 mm diameter window (Fig. 3b, c; Methods). The number of ChR2–GFP-positive
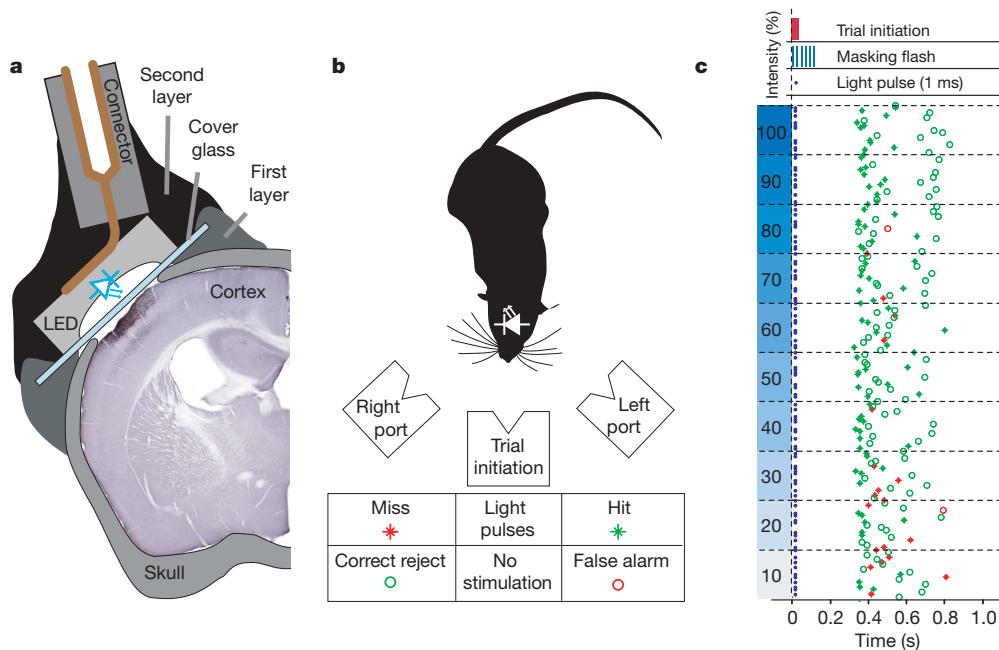

Figure 2 | Photostimulation in freely moving mice performing a detection task. a, Schematic of the photostimulation setup (see Methods). **b**, Schematic of the behavioural apparatus and reward contingencies. The mouse initiates a trial by sticking its snout into the central port. Photostimuli are applied during a stimulation period (300 ms) accompanied by a series of bright blue light flashes delivered to the behavioural arena (30 Hz, 300 ms) to mask possible scattered light from the portable light source. The mouse then decides to enter either the left or the right port for a water reward. If a photostimulus was present, the choice of the left port was rewarded with a drop of water (hit, green star) whereas the choice of the right port lead to a short timeout (4 s, miss, red star). If the stimulus was absent, only the choice of the right port was rewarded with reward (correct reject, green circle) whereas the left port lead to a timeout (4 s, false alarm, red circle). **c**, Data from one session (200 trials) with a single stimulus (1 ms) with decreasing light intensities. Each horizontal line delineates 20 trials at fixed light intensity. Blue dots indicate the presence or absence of a photostimulus. Stimulated and non-stimulated trials were presented pseudo-randomly with a probability of 0.5.

neurons under the photostimulation window correlated with the performance of individual animals.

For each animal we then estimated the number of active neurons as a function of normalized intensity (I_o = intensity/I_{max}) as:

$$N_a(I_o) = \sum_{k \forall \text{cells}} f(I_o i(r_k)) \quad (1)$$

Here r_k is the horizontal position of the kth ChR2–GFP-positive cell and f is the fraction of ChR2-positive cells activated at intensity $I_o i$ (Fig. 1h). $i(r)$ is the spatial distribution of the normalized light intensity in the tissue (horizontal full-width at half maximum = 2.17 mm, 250 μm below the pia) (Supplementary Methods; Supplementary Fig. 5). For trains of five action potentials, an average of 61 neurons (range 6–197) was sufficient to drive reliable performance (more than 65% of correct choices), whereas 297 (range 135–381) active neurons were required with single action potentials (Fig. 3d). The total number of action potentials required for a given level of performance was independent of the stimulus pattern (Supplementary Fig. 6).

Two factors make us believe that our estimates of the number of active neurons should be interpreted as an upper bound. First, the measured spatial distribution of light in the tissue is likely broader than the actual distribution of light (see Supplementary Methods). Second, we did not consider possible deterioration of the optical path (thickening of the dura, bone growth, and so on) over the long timescales required for the behavioural experiments compared

with the more favourable conditions of the calibration measurements. Therefore the actual number of activated neurons in the behavioural experiments might have been lower than the numbers cited above.

Not surprisingly, triggering more action potentials yields better detection accuracy (Fig. 3d). However, performance reached asymptotic levels at remarkably low numbers of directly activated neurons; the range between minimal detection and saturating performance was only a few hundred neurons.

Activated ChR2–GFP-positive neurons were distributed over most of the barrel cortex, with a smattering in adjacent sensory areas. The activated cortical region contains at least 40,000 layer 2/3 neurons (approximately 2,000 per barrel column, unpublished data) implying that synchronous action potentials in less than 1% of layer 2/3 neurons can be robustly perceived. These data imply that mechanisms exist to read out extremely sparse codes from primary sensory areas[6,20,21]. Because of convergence in the L2/3 → L5 pathway, it is possible that even fewer activated L5 cells could be detected by behaving mice. We also note that the detection threshold could vary considerably based on the state of the animal[6,22].

We have shown that ChR2-based optical microstimulation can be used to dissect the impact of precisely timed action potentials in a few genetically defined neurons on mammalian behaviour. Our data show that the favourable characteristics of ChR2 reported previously *in vitro*[10–12,15,23–25], *in vivo*[18] and in invertebrate systems[24,26]—including the ability to generate precisely timed action potentials—are
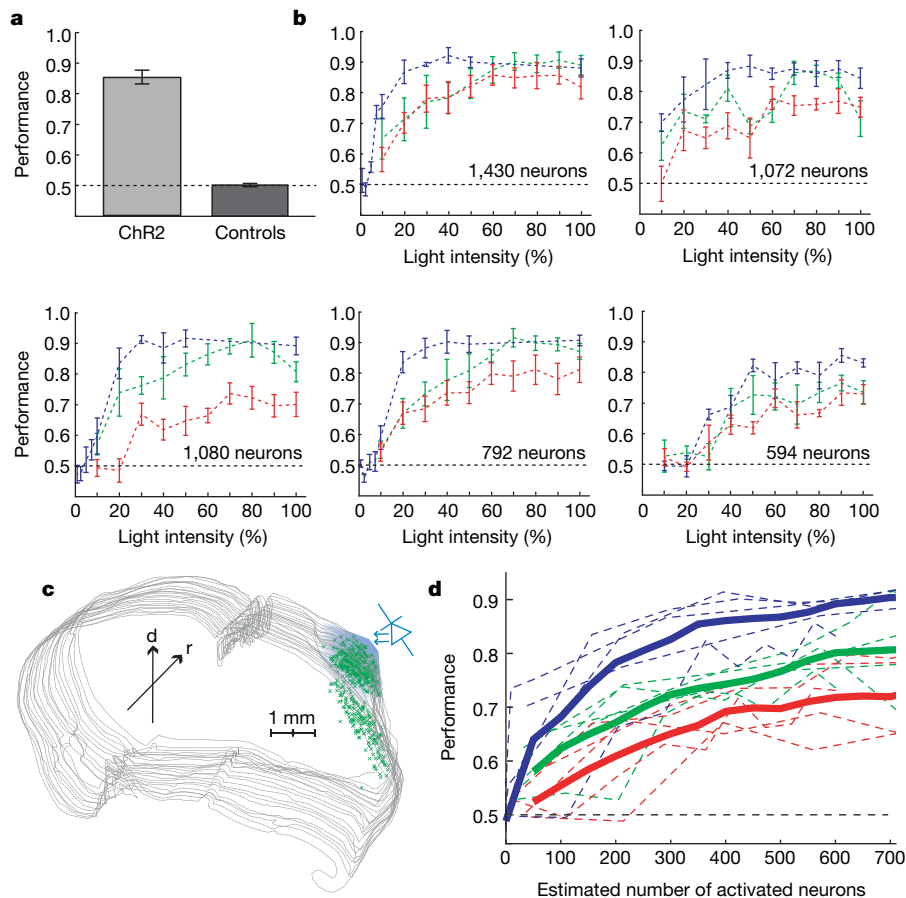

Figure 3 | Behavioural detection of photostimulation. a, Comparison of the performance ((hits + correct rejections)/total trials) in mice expressing ChR2–GFP ($n = 9$) and control mice ($n = 6$) after training with five photostimuli ($P < 0.001$, t-test). **b,** Performance as a function of light intensity (as percentage of $I_{max} = 11.6$ mW mm^{-2}) for five light pulses (1 ms, 20 Hz, blue lines), two light pulses (1 ms, 20 Hz, green lines) and a single light pulse (1 ms, red lines). Dotted lines: mean across five sessions (200–1000 trials per session). Error bars: binomial standard error. The number of ChR2–GFP-positive neurons located under the window area is indicated for each mouse. **c,** Location of ChR2-expressing neurons in serial reconstruction of the sectioned brain (coronal sections). The blue cone illustrates the light source over the window. Arrows indicate rostral (r) and dorsal (d) orientation. **d,** Performance as a function of the number of activated neurons. Thick lines, mean performance across all five animals for one (red), two (green) and five (blue) light pulses. Dotted lines indicate mean values of individual animals from Fig. 3b.

maintained in awake conditions and can be used effectively to drive learning and behaviour.

Photostimulation of genetically defined neurons[27] has key advantages compared with electrical microstimulation. Under typical experimental conditions, electrical microstimulation excites axons non-discriminately, probably including diverse local and long-range axons[7,8]. Therefore, the cell type and cell location that drive behaviour in classical microstimulation experiments are poorly defined. Photostimulation of genetically defined neural populations naturally overcomes these problems. Our estimates of the number of directly activated cortical neurons necessary to drive perception is lower than previous estimates based on electrical microstimulation[28,29]. Our stimuli might be functionally more potent because a pure population of excitatory neurons is activated, whereas electrical microstimulation drives a mixture of diverse excitatory and inhibitory neurons. The robust associative learning induced by ChR2-assisted photostimulation opens the door to study the circuit basis of perception and cognition *in vivo*.

METHODS SUMMARY

***In utero* electroporation.** DNA solution (ChR2–GFP and either mCherry or DsRedexpress ('RFP'); 4:1 molar ratio; final concentration $2 \mu g \mu l^{-1}$) was injected into the right lateral ventricle of embryonic mice (E16). Layer 2/3 progenitor cells were transfected by *in utero* electroporation[14,15].

Photostimulation and behaviour. An imaging window was implanted on the electroporated mice[19] at postnatal day 40–50. A miniature blue high-power LED (470 nm peak wavelength, NFSB036BT, Nichia, Japan) was mounted on the imaging window with black dental acrylic. The timing and intensity of the LED was computer-controlled with a custom-built, low-noise current-source circuit (see Methods). Mice were trained on a detection task to report photostimulation (see Methods). The training protocol consisted of several phases; transitions from one phase to the next were triggered by performance at 65% correct or above. Mice had restricted access to drinking water to maintain 80–85% of their pre-training weight. For calibrations using targeted cell-attached recordings[16] mice were placed under a custom-made two-photon laser-scanning microscope controlled by ScanImage software[19,30]. For the photostimulation the objective was removed and a miniature blue high-power LED (as described above) was placed on the centre of the recording window (see Methods).

Histology. After completion of behavioural experiments, the brain from each animal was cut into coronal or tangential sections (40–60 μm thick) on a cryostat (Leica, CM 3050S). The localization of ChR2–GFP-positive cell bodies was measured using Neurolucida software (MBF Bioscience).

Full Methods and any associated references are available in the online version of the paper at www.nature.com/nature.

1. Penfield, W. & Boldery, P. Somatic motor and sensory representation in the cerebral cortex of man as studied by electrical stimulation. *Brain* **60**, 389–443 (1937).
2. Salzman, C. D., Britten, K. H. & Newsome, W. T. Cortical microstimulation influences perceptual judgements of motion direction. *Nature* **346**, 174–177 (1990).
3. Romo, R., Hernandez, A., Zainos, A. & Salinas, E. Somatosensory discrimination based on cortical microstimulation. *Nature* **392**, 387–390 (1998).
4. Libet, B. in *Handbook of Sensory Physiology* (ed. Iggo, A.) 743–790 (Springer, Berlin, 1973).
5. Leal-Campanario, R., Delgado-Garcia, J. M. & Gruart, A. Microstimulation of the somatosensory cortex can substitute for vibrissa stimulation during Pavlovian conditioning. *Proc. Natl Acad. Sci. USA* **103**, 10052–10057 (2006).
6. Butovas, S. & Schwarz, C. Detection psychophysics of intracortical microstimulation in rat primary somatosensory cortex. *Eur. J. Neurosci.* **25**, 2161–2169 (2007).
7. Tehovnik, E. J. Electrical stimulation of neural tissue to evoke behavioral responses. *J. Neurosci. Methods* **65**, 1–17 (1996).
8. Ranck, J. B. Jr. Which elements are excited in electrical stimulation of mammalian central nervous system: a review. *Brain Res.* **98**, 417–440 (1975).
9. Nagel, G. *et al.* Channelrhodopsin-2, a directly light-gated cation-selective membrane channel. *Proc. Natl Acad. Sci. USA* **100**, 13940–13945 (2003).
10. Boyden, E. S., Zhang, F., Bamberg, E., Nagel, G. & Deisseroth, K. Millisecond-timescale, genetically targeted optical control of neural activity. *Nature Neurosci.* **8**, 1263–1268 (2005).
11. Li, X. *et al.* Fast noninvasive activation and inhibition of neural and network activity by vertebrate rhodopsin and green algae channelrhodopsin. *Proc. Natl Acad. Sci. USA* **102**, 17816–17821 (2005).
12. Ishizuka, T., Kakuda, M., Araki, R. & Yawo, H. Kinetic evaluation of photosensitivity in genetically engineered neurons expressing green algae light-gated channels. *Neurosci. Res.* **54**, 85–94 (2006).
13. Bi, A. *et al.* Ectopic expression of a microbial-type rhodopsin restores visual responses in mice with photoreceptor degeneration. *Neuron* **50**, 23–33 (2006).
14. Hatanaka, Y., Hisanaga, S., Heizmann, C. W. & Murakami, F. Distinct migratory behavior of early- and late-born neurons derived from the cortical ventricular zone. *J. Comp. Neurol.* **479**, 1–14 (2004).
15. Petreanu, L., Huber, D., Sobczyk, A. & Svoboda, K. Channelrhodopsin-2-assisted circuit mapping of long-range callosal projections. *Nature Neurosci.* **10**, 663–668 (2007).
16. Margrie, T. W. *et al.* Targeted whole-cell recordings in the mammalian brain *in vivo. Neuron* **39**, 911–918 (2003).
17. Fee, M. S., Mitra, P. P. & Kleinfeld, D. Central versus peripheral determinants of patterned spike activity in rat vibrissa cortex during whisking. *J. Neurophysiol.* **78**, 1144–1149 (1997).
18. Arenkiel, B. R. *et al. In vivo* light-induced activation of neural circuitry in transgenic mice expressing channelrhodopsin-2. *Neuron* **54**, 205–218 (2007).
19. Gray, N. W., Weimer, R. M., Bureau, I. & Svoboda, K. Rapid redistribution of synaptic PSD-95 in the neocortex *in vivo. PLoS Biol.* **4**, e370 (2006).
20. DeWeese, M. R., Wehr, M. & Zador, A. M. Binary spiking in auditory cortex. *J. Neurosci.* **23**, 7940–7949 (2003).
21. Petersen, R. S., Panzeri, S. & Diamond, M. E. Population coding in somatosensory cortex. *Curr. Opin. Neurobiol.* **12**, 441–447 (2002).
22. Ferezou, I., Bolea, S. & Petersen, C. C. Visualizing the cortical representation of whisker touch: voltage-sensitive dye imaging in freely moving mice. *Neuron* **50**, 617–629 (2006).
23. Zhang, Y. P. & Oertner, T. G. Optical induction of synaptic plasticity using a light-sensitive channel. *Nature Methods* **4**, 139–141 (2006).
24. Nagel, G. *et al.* Light activation of channelrhodopsin-2 in excitable cells of *Caenorhabditis elegans* triggers rapid behavioral responses. *Curr. Biol.* **15**, 2279–2284 (2005).
25. Wang, H. *et al.* High-speed mapping of synaptic connectivity using photostimulation in channelrhodopsin-2 transgenic mice. *Proc. Natl Acad. Sci. USA* **104**, 8143–8148 (2007).
26. Schroll, C. *et al.* Light-induced activation of distinct modulatory neurons triggers appetitive or aversive learning in *Drosophila* larvae. *Curr. Biol.* **16**, 1741–1747 (2006).
27. Lima, S. Q. & Miesenbock, G. Remote control of behavior through genetically targeted photostimulation of neurons. *Cell* **121**, 141–152 (2005).
28. Salzman, C. D., Murasugi, C. M., Britten, K. H. & Newsome, W. T. Microstimulation in visual area MT: effects on direction discrimination performance. *J. Neurosci.* **12**, 2331–2355 (1992).
29. Tehovnik, E. J., Tolias, A. S., Sultan, F., Slocum, W. M. & Logothetis, N. K. Direct and indirect activation of cortical neurons by electrical microstimulation. *J. Neurophysiol.* **96**, 512–521 (2006).
30. Pologruto, T. A., Sabatini, B. L. & Svoboda, K. ScanImage: flexible software for operating laser-scanning microscopes. *Biomed. Eng. Online* **2**, 13 (2003).

Author Contributions D.H. and K.S. designed the experiments. D.H. performed the behavioral and *in vivo* physiological experiments. L.P., D.H. and K.S. performed the brain slice measurements. N.G. performed histology. S.R., T.H., Z.M. and K.S. provided advice and equipment. D.H. and K.S. wrote the paper. All authors discussed the results and commented on the manuscript.

Author Information Reprints and permissions information is available at www.nature.com/reprints. Correspondence and requests for materials should be addressed to K.S. (svobodak@janelia.hhmi.org).

METHODS

All experimental protocols were conducted according to the National Institutes of Health guidelines for animal research and were approved by the Institutional Animal Care and Use Committee at Cold Spring Harbor Laboratory and HHMI Janelia Farm Research Campus.

In utero electroporation. Venus or GFP was fused to the carboxy (C) terminus of the first 315 amino acids of channelrhodopsin-2 (gift from G. Nagel). The construct ('ChR2–GFP') was inserted into pCAGGS vector modified for *in utero* electroporation[19]. DNA was purified and concentrated using Qiagen plasmid preparation kits and dissolved in 10 mM Tris–HCl (pH 8.0). Layer 2/3 progenitor cells were transfected by *in utero* electroporation. E16 timed-pregnant C57BL/6J mice (Charles River, Wilmington, Massachusetts) were deeply anaesthetized by using an isoflurane–oxygen mixture (2% isoflurane/O_2 by volume). The abdomen was opened and the uterine horns were exposed. Approximately 1 μl of DNA solution coloured with Fast Green (Sigma, St. Louis, Missouri) was pressure injected (Picospritzer, General Valve, Fairfield, New Jersey) through a pulled glass capillary pipette (Warner Instruments, Hamden, Connecticut) into the right lateral ventricle of each embryo. The DNA solution contained a mixture of plasmids encoding ChR2–GFP and either mCherry or DsRedexpress ('RFP') in a 4:1 molar ratio, at a final concentration of 2 μg/μl. The DNA was electroporated into the right lateral ventricular wall of the embryo's brain by applying five pulses of 45 V (duration 50 ms, frequency 1 Hz) through a pair of custom-made tweezer-electrodes, with the positive plate contacting the right side of the head. Approximately 50% of the surviving pups were strongly positive for transgene expression.

Photostimulation. A chronic imaging window was implanted on the electroporated mice at postnatal age 40–50 days. The mice were anaesthetized by using an isoflurane-oxygen mixture (2% isoflurane/O_2 by volume) delivered by an anaesthesia regulator (SurgiVet, Waukesha, Wisconsin) and mounted on a stereotaxic frame (Stoelting, Wood Dale, Illinois). The animals were screened through the exposed skull for expression of RFP by using a fluorescent dissecting scope (MVX10, Olympus, Tokyo, Japan). Expression centred on the barrel cortex was found in about 30% of the positive mice. A thin cover of cyanoacrylate adhesive (Vetbond, 3M, St Paul, Minnesota) was applied to allow subsequent adhesion of the dental acrylic. A 2 mm diameter skull flap overlying right barrel cortex (centred on 1.5 mm caudal, 3.5 mm lateral of bregma) was removed by using a fine motorized drill. Special care was taken to leave the dura intact. The opening was covered with a thin layer of warm 1% agarose (Sigma, St Louis, Missouri), and a 5 mm diameter round cover glass (Warner Instruments, Hamden, Connecticut) was sealed on top of the agarose with black dental acrylic (Lang Dental, Wheeling, Illinois). A titanium bar was embedded rostral to the window above the midline to allow fixation to the microscope. After the initial surgery, the animals were left to recover for five days. Animals of the same age that were not electroporated were used as controls. A miniature blue high-power LED (470 nm peak wavelength, NFSB036BT, Nichia, Tokyo, Japan) was mounted on the imaging window. The assembly was then covered with black dental acrylic to prevent leakage of light. The timing and intensity of the LED was computer-controlled with a custom-built, low-noise current-source circuit. All LEDs were tested before implantation and after termination of the experiments.

The distribution of light intensity at the surface of the brain was measured using a beam profiler (Supplementary Methods; Supplementary Fig. 5a, b). The distribution of light intensity in the brain, which was used to estimate the number of activated neurons (equation (1)), was estimated in a block of freshly cut brain. The dorsal surface, with mounted skull and LED, was on the side. The cut surface was imaged from the top by using a CCD (charge-coupled device) (Supplementary Fig. 5). Because the light that reaches the camera is smeared by scattering on its way out of the tissue, the width of the distribution (Supplementary Fig. 5c) on the cut surface is likely an overestimate of the actual width of the distribution in the brain.

In vivo two-photon imaging and cell-attached recordings. For targeted cell-attached recordings, similar surgery was performed as described except that the skull opening was only 1.5 mm and a custom-shaped semilunar cover-glass was sealed in place using dental acrylic, leaving the lateral edge of the exposed dura accessible to the recording electrode. To monitor the level of anaesthesia, an electrocorticogram was recorded by inserting a thin Teflon-coated silver wire between the dura and skull in the contralateral hemisphere. A reference wire was inserted above the cerebellum. *In vivo* imaging was performed by using a custom-made two-photon laser-scanning microscope controlled by ScanImage software[19,30]. The light source was a pulsed Ti:sapphire laser (wavelength, 920–1010 nm; power, 50–200 mW in the objective back-focal plane; MaiTai, Spectra-Physics, Mountain View, California). Red and green fluorescence photons were separated by using a 565 nm dichroic mirror (Chroma Technology, Brattleboro, Vermont) and barrier filters (green, BG22;

red, 607/45; Chroma). Signals were collected using photomultiplier tubes (3896, Hamamatsu, Hamamatsu City, Japan). We used an objective lens (×40, 0.8 NA) from Olympus (Tokyo, Japan). RFP-positive neurons were targeted for loose seal cell-attached recordings by using the two-photon fluorescence image[16]. The recording pipette contained (in mM): 10 KCl, 140 K-gluconate, 10 HEPES, 2 $MgCl_2$, 2 $CaCl_2$, 0.05 sulphorhodamine 101, pH 7.25, 290 milli-osM. The signals were recorded using a patch clamp amplifier (Axoclamp 200B, Axon Instruments, Foster City, California). For the photostimulation, the objective was removed and a miniature blue high power LED (470 nm) was placed on the centre of the recording window. To determine the spike threshold, single light pulses of 1 ms or 10 ms duration were initially presented at maximal intensity. In addition, a series of longer pulses (20–100 ms) were tested for each recording without revealing any additional responsive neurons. All neurons in the analysis displayed evoked or spontaneous activity. If a neuron fired with a 1 ms pulse, the threshold was probed by presenting varying light intensity. The light pulses were presented every 15 s with increasing amplitude. Six to ten intensity values were repeated five times for each condition. Data collection and LED stimulation were controlled by custom-written physiology software in MATLAB (Mathworks, Natick, Massachusetts). All data of neurons responding to light durations above 1 ms were pooled for the analysis.

Training procedures. Mice with implanted LEDs had free access to food but had restricted access to drinking water to maintain 80–85% of their pre-training weight. Water was only available during and immediately after the behavioural sessions, with a minimum of 1.5 ml per day. Body weight was monitored daily before the training. The mice were kept at a reversed 12 h light/dark cycle and sessions were performed during the dark cycle. The behavioural box consisted of a white Plexiglas chamber (200 mm × 140 mm × 200 mm) with three ports mounted on one wall. The ports were conical and equipped with an infrared phototransistor–photodiode pair that signalled the interruption of the beam when the mouse entered his snout. The floor was a washable plastic kitchen cutting board. Both box and floor were cleaned with 70% ethanol after each animal. The box was placed in a sound- and light-proof cabinet that was constantly illuminated with bright white light. The box was covered with a transparent Plexiglas plate in which an infrared camera (for monitoring) and a bright masking light (high-power blue LED 470 nm, Luxeon V, Lumileds, San Jose, California) were mounted along the midline. The white light illumination of the behavioural box and the bright blue light flash were designed to mask any scattered light potentially reaching the retina through the skull or brain. The masking flash consisted of a series of bright 2 ms flashes (30 Hz, for 300 ms) illuminating the entire box. This mask flash was presented during every stimulation period (independently of whether a stimulus was presented).

Detection task. Training consisted of several phases. Transitions from one phase to the next were triggered by performance at 65% correct or above.

1. Mice were habituated to the behavioural box and trained for one week to get water from either left or right water port by breaking the light beam inside the port. The availability of water in a port was signalled with a white noise click from a loudspeaker (synchronized with the 5 ms valve opening). Water was delivered with a gravitational system and the drop size was controlled with solenoid valves (Neptune Research, West Caldwell, New Jersey). Single drop volume was approximately 4 μl. All components of the behaviour box were controlled with custom MATLAB software that was interfaced with a real-time processor system (RP2 or RM1, Tucker-Davis Technologies, Gainesville, Florida).

2. The snout of the mouse had to enter the centre port (trial initiation) to make water reward available in either the left or the right port for 10 s.

3. The LED was connected to the behavioural control system before the mouse was placed in the box. The cable to the LED controller ran through a hole in the Plexiglas cover and was mounted on a rotating hook 60 cm above the mouse. Reward was only available in the left port after photostimulation, whereas water was available on the right port in the absence of photostimulation (Fig. 2b). Stimuli were presented in an interleaved series of 20 trials, with each type occurring with a probability of 0.5 (pseudo-randomly, excluding runs of more than four consecutive identical trials). Occasional response bias for one port over the other was corrected by repeating the stimulus associated with the ignored port until the correct response was achieved.

4. Animals were trained to respond to fewer stimuli and decreased light intensity.

Histology. After completion of behavioural experiments, the mice were deeply anaesthetized and transcardially perfused with 4% paraformaldehyde in 0.1 M phosphate buffer, pH 7.4. The brain was carefully removed from each animal and cut into coronal or tangential sections ranging from 40 to 60 μm on a cryostat (CM 3050S, Leica Microsystems, Wetzlar, Germany). ChR2–GFP-positive neurons were detected with an anti-GFP polyclonal antibody (Rb-anti-GFP, AB3080P, dilution 1:700, Chemicon, Temecula, California), subsequently amplified with a biotin-conjugated antibody (Gt-anti-Rb, 111-066-003, Jackson

ImmunoResearch Laboratories, West Grove, Pennsylvania) and revealed by using a standard ABC-kit (Vector Laboratories, Burlingame, California) with diaminobenzidine (DAB) precipitation. The sections were then mounted, dehydrated with increasing alcohol series, and coverslipped in DPX mounting medium. The localization of the cell bodies and serial reconstruction of the brain volume was performed in Neurolucida software (MBF Bioscience, Williston, Vermont). Estimates of the number of neurons under the window area were performed in MATLAB by calculating the number of neurons inside a sphere of diameter 2 mm positioned above the window centre. To define the degree of co-localization of ChR2–GFP and RFP, the ChR2–GFP was revealed with a fluorescent anti-GFP antibody (Rb-anti-GFP-488, A21311, Invitrogen, Carlsbad, California) whereas the cytosolic red signal was detected directly. Thick sections (40 μm) were imaged under a confocal microscope (LSM 510, Carl Zeiss, Jena, Germany). The individual red or green neurons were then classified and counted by hand on the image stacks using Object-Image software (http://simon.bio.uva.nl/object-image.html). Based on *in vivo* two-photon imaging or confocal and bright field microscopy of fixed brain sections, we could not detect any morphological changes due to the expression of ChR2 in layer 2/3 neurons.